Science of the Total Environment 656 (2019) 373–387

Contents lists available at ScienceDirect

Science of the Total Environment

journal homepage: www.elsevier.com/locate/scitotenv

Effects of temperature, precipitation and carbon dioxide concentrations on the requirements for crop irrigation water in China under future climate scenarios

Yajie Zhang [a], Yanfen Wang [b], Haishan Niu [a,*]

[a] College of Resources and Environment, University of Chinese Academy of Sciences, No.19A Yuquan Road, Beijing, China
[b] College of Life Sciences, University of Chinese Academy of Sciences, No.19A Yuquan Road, Beijing, China

HIGHLIGHTS

- We predict the changes in irrigation water requirement for four crops in China.
- The irrigation water requirements for crops are dominated by various climatic factors.
- The irrigation water requirements under RCP8.5 reduce mainly by the CO_2 effect.
- Northwestern China always requires vast amounts of irrigation water for crops.

GRAPHICAL ABSTRACT

Irrigation water requirements with temperature-only (T-only), precipitation-only (P-only) and carbon dioxide-only (CO_2-only) for (a) maize, (b) rice, (c) soybean and (d) wheat under the representative concentration pathway scenario RCP8.5 in China in the 2010s (2006–2020), 2030s (2021–2040), 2050s (2041–2060), 2070s (2061–2080), and 2090s (2081–2100).

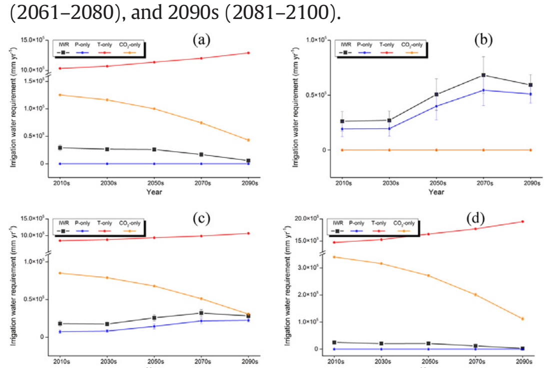

ARTICLE INFO

Article history:
Received 29 May 2018
Received in revised form 18 November 2018
Accepted 24 November 2018
Available online 26 November 2018

Editor: Ralf Ludwig

Keywords:
Atmospheric CO_2 concentrations
Crop irrigation water requirements
Representative concentration pathways
China

ABSTRACT

Maize, rice, wheat and soybean—the major staple food crops in China—have a crucial role in national food security and economic development. Predictions of changes in the requirements for irrigation water in food crop production under climate change may provide scientific support for the optimum allocation of water resources and measures to mitigate climate change. We conducted a spatial grid-based analysis using projections of future climate generated by a bias-correction and spatial disaggregation multi-model ensemble for three representative concentration pathway scenarios (RCP2.6, RCP4.5 and RCP8.5) adopted by the fifth phase of the Coupled Model Intercomparison Project. We investigated the effects of climate change associated with increasing temperature, changed precipitation and increased concentrations of atmospheric carbon dioxide (CO_2) on the irrigation water requirements of maize, rice, wheat and soybean in China at the end of the 21st century (2081–2100). Our results indicate that the irrigation water requirements of maize and wheat are driven by temperature and especially by CO_2 concentrations in the northwest interior area as a result of the low rainfall and high rates of evaporation; the irrigation water requirement of soybean is influenced by a combined effect of temperature, precipitation and CO_2 concentration, whereas the irrigation water requirement for rice is dominated by precipitation alone in the southern coastal region, which has high rainfall. The irrigation water requirements of crops

* Corresponding author at: College of Resources and Environment, University of Chinese Academy of Sciences, No.19A Yuquan Road, Beijing, 100049, China.
E-mail address: niuhs@ucas.ac.cn (H. Niu).

https://doi.org/10.1016/j.scitotenv.2018.11.362

decrease mainly as a result of the beneficial effects of CO_2 on plant growth in China. The regions requiring vast amounts of irrigation water as a result of climate change are mainly concentrated in northwestern China. The effects of climate change affect the requirement for irrigation water, especially under high-emission scenarios, and should be studied further to design appropriate adaptation strategies for the management of agricultural water to maintain the sustainable development of agriculture.

1. Introduction

Irrigation has a major role in food security and the alleviation of poverty in China. Over 70% of the water consumed in China is used for agricultural irrigation, with irrigation water applied to >75% of crops on >30% of agricultural land (Thomas, 2008; Xiong et al., 2009). As irrigation is the major use of water in agricultural regions, the capacity to supply irrigation water is crucial in the long-term development of water resources and in decision-making about future agricultural production in China.

The irrigation water requirement (IWR) is the amount of water that must be supplied to a crop via irrigation to achieve optimum crop growth, taking into consideration the losses incurred during the transport and application of the irrigation water. Global factors such as climate change [i.e., increasing temperatures, fluctuations in precipitation and increasing concentrations of atmospheric carbon dioxide (CO_2)] are placing increasing stress on agricultural systems and drive variations in the IWR (Wang et al., 2014).

A number of studies over the past few decades have quantified the impact of future climate change on irrigation at regional and global scales. Significant increases have been estimated for the long-term IWR as a result of a warming climate and increased evaporative demand (e.g., Fischer et al., 2007; Pfister et al., 2011; Konzmann et al., 2013; Elliott et al., 2014). Increased atmospheric concentrations of CO_2 have been shown to directly affect transpiration via both the physiological and structural responses of plants, which tend to reduce their leaf stomatal conductance and thus the rate of evapotranspiration, improving the efficiency of water use by crops (Gerten et al., 2007; Hatfield et al., 2011). Therefore quantifying and analyzing the spatial and temporal characteristics of the regional demand for irrigation water by agriculture is important in developing strategies for water management under the future impacts of climate change and the associated demographic, socioeconomic and technological changes.

Assessments of the geographical distribution of crop water requirements in China are widely available (e.g., Leng and Tang, 2014). However, data on the extent to which variations in temperature, precipitation and atmospheric CO_2 concentrations will affect future IWRs for specific crops start later and are fairly sparse. Some studies do not take into account the use of water by specific crops. For example, Thomas (2008) modeled the effects of climate change on irrigation requirements in China with high-resolution gridded climate datasets; but he identified the crops as main, second and third crops according to the cropping system. Some studies take into account the specific field crops without consideration of the effect of CO_2 on the use of water by crops. For example, Liu et al. (2009) provided IWRs for 30 different crops estimated using the Food and Agriculture Organization (FAO) Penman–Monteith equation and the crop coefficient method based on meteorological data for the period 1970–2000 from observation stations and statistical data about the stages of crop growth in different areas of China. Cong et al. (2011) reported increases in the IWRs of crops in China due to increases in future temperatures using the FAO Penman–Monteith equation, crop coefficients and the Köppen climate classification system under future emission scenarios.

To improve these methods and to fill some gaps in research, this study applied a standard method of estimating future IWRs (including the crop coefficient approach and the FAO Penman–Monteith equation incorporating the effect of CO_2) based on gridded climatic data from 2006 to 2100 simulated by six bias correction and spatial disaggregation climate projections in the fifth phase of the Coupled Model Intercomparison Project (CMIP5) archive under three representative concentration pathway (RCP) scenarios (RCP2.6, RCP4.5 and RCP8.5). The aims of this study were to: (1) explore the long-term temporal and spatial variations in the IWR of major crops (maize, rice, wheat and soybean) in China in the future; (2) conduct an analysis of how the IWR responds to climate change associated with variations in temperature, precipitation and CO_2 concentrations; and (3) investigate the dominant climatic factors governing the behavior of the crop-specific IWRs. The results were compared with historical publications to determine the validity and precision of this method. These results may provide reference values for climate adaptation strategies and the sustainable development of agriculture under scenarios of climate warming and water shortages. The method developed in this study may also provide guidance for the scientific research in agro-climatology and the establishment of reasonable agricultural irrigation schemes.

2. Data and methodology

2.1. Crop types

Cereal and legume crops—such as maize (*Zea mays* L.), rice (*Oryza sativa* L.), wheat (*Triticum aestivum* L.) and soybean (*Glycine max* L.)—are cultivated and produced in most cropland areas in China (http://data.stats.gov.cn) (Leff et al., 2004). The majority of the cropland areas are in southern and eastern China in the humid, rainy, monsoon climate zone, although a few are located in the dry area of northwest China. Potential changes in the IWRs for these four crops are important in assessing the impact of climate change on agricultural production in China.

2.2. Future climate scenarios

The future scenarios used to produce the simulations are four of the RCPs developed for IPCC AR5 and designed to simulate projected changes in climate due to changes in greenhouse gas emissions, aerosol concentrations, ozone concentrations and land use (Moss et al., 2010; Taylor et al., 2012). Of the four RCPs, RCP2.6 is a peak-and-decline scenario that first reaches radiative forcing at around 3.1 W m^{-2} by the mid-21st century and returns to 2.6 W m^{-2} by 2100; RCP4.5 is a scenario that stabilizes radiative forcing at 4.5 W m^{-2} in the year 2100 without ever exceeding that value; and RCP8.5 is a so-called baseline scenario representing the highest levels of radiative forcing (up to 8.5 W m^{-2}) and changes in greenhouse gas concentrations (>1370 ppm CO_2 equivalent) (Moss et al., 2010; van Vuuren et al., 2011; Zhang et al., 2017). We selected RCP2.6, RCP4.5 and RCP8.5 to highlight the impact of climate change on the spatiotemporal patterns of irrigation in China under scenarios with different greenhouse gas emissions.

2.3. Calculation of crop irrigation requirements

The Penman–Monteith equation and crop coefficient approach recommended by the FAO are used to calculate the IWRs of crops. The

Penman–Monteith equation has a good physical basis and has been widely used as a model to estimate crop water requirements and to design and operate irrigation schemes (Allen et al., 1998). To account for losses due to inefficiencies in irrigation, the IWR during the growing season is estimated using the equations (Döll and Siebert, 2002; Shen et al., 2013):

$$IWR = \frac{ET_c - P_e}{I_c} \tag{1}$$

$$ET_c = K_c \cdot ET_0 \tag{2}$$

where *IWR* is the irrigation water requirement of a particular crop (mm day^{-1}), ET_0 is the reference evapotranspiration (mm day^{-1}), ET_c is the crop-specific evapotranspiration (mm day^{-1}), which depends on the growing stage of the crop and used to quantify crop water requirement, K_c is the crop coefficient and represents important parameters for irrigation scheduling and water allocation, P_e is the effective rainfall (i.e., the rainfall transferred to the soil moisture content) (mm day^{-1}) and I_c is the irrigation efficiency taking into consideration the water lost during the diversion from river channels and reservoirs to the field (Shen et al., 2013).

The IWR varies widely and is determined by factors such as the crop variety, the soil properties, the aquifer and weather conditions, the water conveyance conditions and local management practices (e.g., sowing date, growth period and water flooding) (Bortolini et al., 2018). It is known that there are different methods of irrigating rice in China (Yao et al., 2014): (1) conventional paddies, where ponding is deep at about 10 cm; (2) shallow-ponded water paddies, where the ponding depth is close to 5 cm; (3) intermittent flooding, where the climate allows the growth of aerobic rice; and (4) permanent soil wetting, such as on the plain south of the Yangtze River. Maize, wheat and soybean may be grown with full irrigation (e.g., in the upper Yellow River Basin) or with irrigation only as a supplement to rainfall (e.g., on the North China Plain) (Fang et al., 2010). Each type of system has different irrigation requirements. In this study, conventional irrigation only as a supplement to rainfall is considered as the IWR to represent the minimum requirement for irrigation water. The soil water storage, capillary rise and leaching fraction and requirements (for improving the hydraulic properties of the soil or leaching salts) are assumed to be zero.

2.3.1. Reference evapotranspiration

The reference evapotranspiration (ET_0) can be estimated from the meteorological variables (with some simplifications) and can therefore be used in different regions (Allen et al., 1998). For a hypothetical reference crop, the daily ET_0 is calculated based on the FAO-56 Penman–Monteith method (Allen et al., 1998). Considering the variation in the stomatal conductance with atmospheric CO_2 concentrations, ET_0 is calculated using the following equation referred to Fares et al. (2016):

$$ET_0 = \frac{0.408\Delta(R_n - G) + \gamma \frac{900}{T+273} u_2 (e_s - e_a)}{\Delta + \gamma\left(1 + \frac{r_s}{r_a}\right)} \tag{3}$$

where ET_0 is the reference evapotranspiration (mm day^{-1}), R_n is the net radiation at the crop surface (MJ m^{-2} day^{-1}), G is the soil heat flux density (MJ m^{-2} day^{-1}), T is the mean daily air temperature at 2 m height (°C), e_s is the saturation vapor pressure (kPa), e_a is the actual vapor pressure (kPa), $e_s - e_a$ is the saturation vapor pressure deficit (kPa), Δ is the slope of the vapor pressure curve (kPa °C^{-1}), γ is the psychrometric constant (kPa °C^{-1}), r_s is the bulk surface resistance (s m^{-1}), r_a is the aerodynamic resistance (s m^{-1}) and u_2 is the wind speed at 2 m height (m s^{-1}).

In this study, ET_0 is calculated using the Penman–Monteith method where input variables are modeled as proposed by Allen et al. (1998) and widely reported to give reliable estimates (e.g., Raziei and Pereira, 2013; Pandey and Pandey, 2016; Almorox et al., 2018). In this method, the daily values of the e_s, e_a, R_n, G, Δ and γ data and the associated intermediate parameters that could not be provided by global climate models (GCMs) are estimated empirically from the maximum and minimum temperatures, the altitude above sea-level and the latitude of different grids. In addition, by modifying the stomatal conductance term according to the increased CO_2 concentrations, the Penman–Monteith model can also be used to evaluate the impact of CO_2 enrichment on

Table 1
Parameters used in the reference evapotranspiration equations of the Penman–Monteith method, which incorporates the effect of carbon dioxide on crop growth [modified from Zhang et al., 2018b].

	Parameter	Equation
1	z: elevation above sea level (m)	
2	P: atmospheric pressure (kPa)	$P = 101.3(\frac{293-0.0065z}{293})^{5.26}$
3	γ: psychrometric constant (kPa °C^{-1})	$\gamma = 0.665 \times 10^{-3} \times P$
4	T_{mean}: average air temperature (°C)	$T_{mean} = \frac{T_{min}+T_{max}}{2}$
5	$e^0(T)$: saturation vapor pressure (kPa)	$e^0(T) = 0.6108e^{(\frac{17.27T}{T+237.3})}$
6	e_s: mean saturation vapor pressure (kPa)	$e_s = \frac{e^0(T_{max})+e^0(T_{min})}{2}$
7	Δ: slope of saturation vapor pressure curve (kPa °C^{-1})	$\Delta = \frac{4098[0.6108e^{(\frac{17.27T_{mean}}{T_{mean}+237.3})}]}{(T_{mean}+237.3)^2}$
8	e_a: actual vapor pressure (kPa)	$e_a = 0.6108e^{\{\frac{17.27[T_{min}-(0\sim4)]}{[T_{min}-(0\sim4)]+237.3}\}}$
9	R_a: extraterrestrial radiation (MJ m^{-2} d^{-1})	$R_a = 37.6d_r[w_s \sin(\varphi)\sin(\delta) + \cos(\varphi)\cos(\delta)\sin(w_s)]$
10	φ: latitude (rad)	
11	d_r: inverse relative distance Earth-Sun	$d_r = 1 + 0.033\cos(\frac{2\pi}{365}J)$
12	δ: solar declination (rad)	$\delta = 0.409\sin(\frac{2\pi}{365}J - 1.39)$
13	J: number of the day in the year	
14	ω_s: sunset hour angle (rad)	$\omega_s = \cos^{-1}[-\tan(\varphi)\tan(\delta)]$
15	R_s: solar radiation (MJ m^{-2} d^{-1})	$R_s = (0.16 \sim 0.19) \times R_a \times \sqrt{T_{max} - T_{min}}$
16	R_{ns}: net solar radiation (MJ m^{-2} d^{-1})	$R_{ns} = 0.77R_s$
17	R_{so}: clear-sky solar radiation (MJ m^{-2} d^{-1})	$R_{so} = (0.75 + 2 \times 10^{-5}z) \times R_a$
18	R_{nl}: net longwave radiation (MJ m^{-2} d^{-1})	$R_{nl} = 4.903 \times 10^{-9} \times [\frac{(T_{min}+273.16)^4+(T_{max}+273.16)^4}{4}](0.34-0.14\sqrt{e_a})[\frac{1.35R_s}{R_{so}}-0.35]$
19	R_n: net radiation (MJ m^{-2} d^{-1})	$R_n = R_{ns} - R_{nl}$
20	G: soil heat flux (MJ m^{-2} d^{-1})	$G_{month,\,i} = 0.14(T_{month,\,i} - T_{month,\,i-1})$; $T_{month,i}$ refers mean air temperature of month i (°C)
21	u_2: wind speed (m s^{-1})	~2

Table 2
Default indications for maize, rice, soybean and wheat provided by Allen et al. (1998) and Dam and Malik (2003). The crop coefficients, $K_{c\ mid}$ and $K_{c\ end}$, should be adjusted for climate.

Crop type	Length of the initial growth stage (d)	Kc ini	Length of the crop development stage (d)	Length of the mid-season stage (d)	Kc mid	Mean crop height in the mid-season stage (m)	Length of the late season stage (d)	Kc end	Mean crop height in the late season stage (m)
Maize	30	0.30	40	50	1.20	1.60	50	0.60	2.00
Rice	30	1.10	30	60	1.20	0.90	30	0.75	1.00
Soybean	20	0.40	30	60	1.15	0.65	25	0.50	0.80
Spring wheat	30	0.30	140	40	1.15	0.85	30	0.30	1.00
Winter wheat	30	0.70	140	40	1.15	0.85	30	0.30	1.00

Table 3
Details of the six CMIP5 coupled models used in this study.

Model acronym	Institute	Origin resolution (longitude × latitude) (°)
CanESM2	Canadian Centre for Climate Modeling and Analysis, Canada	~2.8 × 2.8
CCSM4	National Center for Atmospheric Research, USA	1.25 × 0.9
CSIRO-Mk3-6-0	Commonwealth Scientific and Industrial Research Organization, Australia	1.875 × 1.875
GISS-E2-R	NASA Goddard Institute for Space Studies, USA	2.5 × 2
IPSL-CM5A-LR	Institut Pierre-Simon Laplace, France	3.75 × 1.875
MPI-ESM-LR	Max-Planck Institute for Meteorology, Germany	1.875 × 1.875

ET_0; this has previously been verified worldwide (Islam et al., 2012; Fares et al., 2016; Wang et al., 2018).

To account for the effects of CO_2 on ET_0, the ratio r_s/r_a, which is a function of the wind speed at 2 m height, is modified according to the variations in CO_2 concentrations for a grass reference surface (Stockle et al., 1992; Allen et al., 1998):

$$r_s = \frac{1}{g\left[(1+p)-p\left(\frac{[CO_2]}{330}\right)\right]} \times \frac{1}{12h\left[1+\frac{7}{100}\left(\frac{[CO_2]-330}{330}\right)\right]} \quad (4)$$

$$r_a = \frac{208}{u_2} \quad (5)$$

where g is the reference stomatal conductance without the effect of CO_2 for the reference crop of grass here supposed equal to 0.01 m s^{-1} as reported by Fares et al. (2016), p is the percentage decrease in stomatal conductance specific to the vegetation type (p is 40% if the land cover type is the crop), $[CO_2]$ is the atmospheric CO_2 concentration (ppm) and 330 represents the baseline atmospheric CO_2 concentration (ppm), h is the height of the reference crop of grass (0.12 m) and u_2 is the wind speed at 2 m height (m s^{-1}). The acceptable range of CO_2 concentrations in these equations is valid and covers most of the projected ranges of CO_2 concentration for the RCP scenarios by the year 2100 (Stockle et al., 1992; Islam et al., 2012).

Details of the modified ET_0 input parameters applied in this study are given in Table 1; see Allen et al. (1998), Raziei and Pereira (2013) and Fares et al. (2016) for more detail.

2.3.2. Crop coefficient during the growing period

The crop coefficient (K_c) is the ratio between the evapotranspiration of well-watered crops and ET_0 (ET_c/ET_0), which reflects the relative water consumption capacity of different crops during different stages of growth. In general, K_c is supposed to vary during the four stages of crop development: the initial growth period; the rapid development period; the mid-season period; and the late season period. We used the

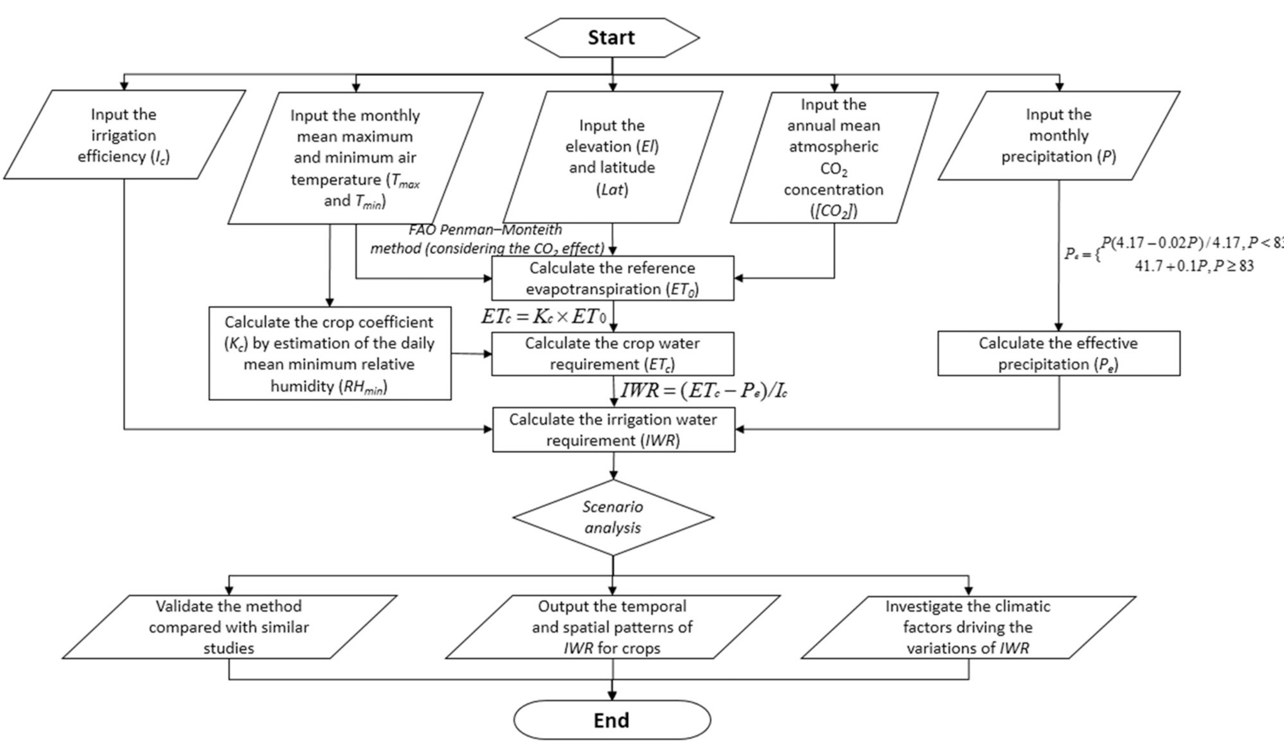

Fig. 1. Calculation procedure for the irrigation water requirement (IWR) for crops in China from 2006 to 2100.

default indications for crops given by Allen et al. (1998) adjusted for climate. These values were validated and shown to be close to the values estimated in China from experimental data (Table 2) (Liu and Pereira, 2000):

$$K_c = K_{c\ tab} + [0.04(u_2-2)-0.004(RH_{\min}-45)]\left(\frac{h}{3}\right)^{0.3} \tag{6}$$

$$RH_{\min} = \frac{0.6108e^{\left(\frac{17.27[T_{\min}-(0\sim4)]}{[T_{\min}-(0\sim4)]+237.3}\right)}}{0.6108e^{\left(\frac{17.27T_{\max}}{T_{\max}+237.3}\right)}} \times 100 \tag{7}$$

where $K_{c\ tab}$ is the K_c value (for $K_{c\ mid}$ and $K_{c\ end}$) tabulated by Allen et al. (1998) for maize, rice, soybean and wheat (including both spring and winter wheat), u_2 is the mean value of the daily wind speed at 2 m height over grass (m s^{-1}), $RH_{\min}$ is the mean value of the daily minimum relative humidity (%) and h is the mean plant height during the mid- or late growing stage (m) (Table 2). $RH_{\min}$ can be calculated on an average monthly basis from Eq. (7), where $T_{\min}$ and $T_{\max}$ are the mean daily minimum and maximum air temperatures during the corresponding growth stage (°C) (Liu and Pereira, 2000).

The global crop calendar dataset for major crops published by Sacks et al. (2010) was adopted and assumed to be stable until the end of the 21st century. This dataset of crop calendars (http://nelson.wisc.edu/sage/data-and-models/crop-calendar-dataset/index.php; last accessed December 2010) was compiled by digitizing and geo-referencing existing observations for the start and end of cropping periods from data supplied by the US Department of Agriculture and the FAO for China. The calendars for maize, soybean, rice (main season), rice 2 (second season), wheat and winter wheat were all considered in this study.

2.3.3. Effective rainfall

The effective rainfall P_e on agricultural land is defined as the portion of rainfall and snowmelt penetrating the canopy, infiltrating into the

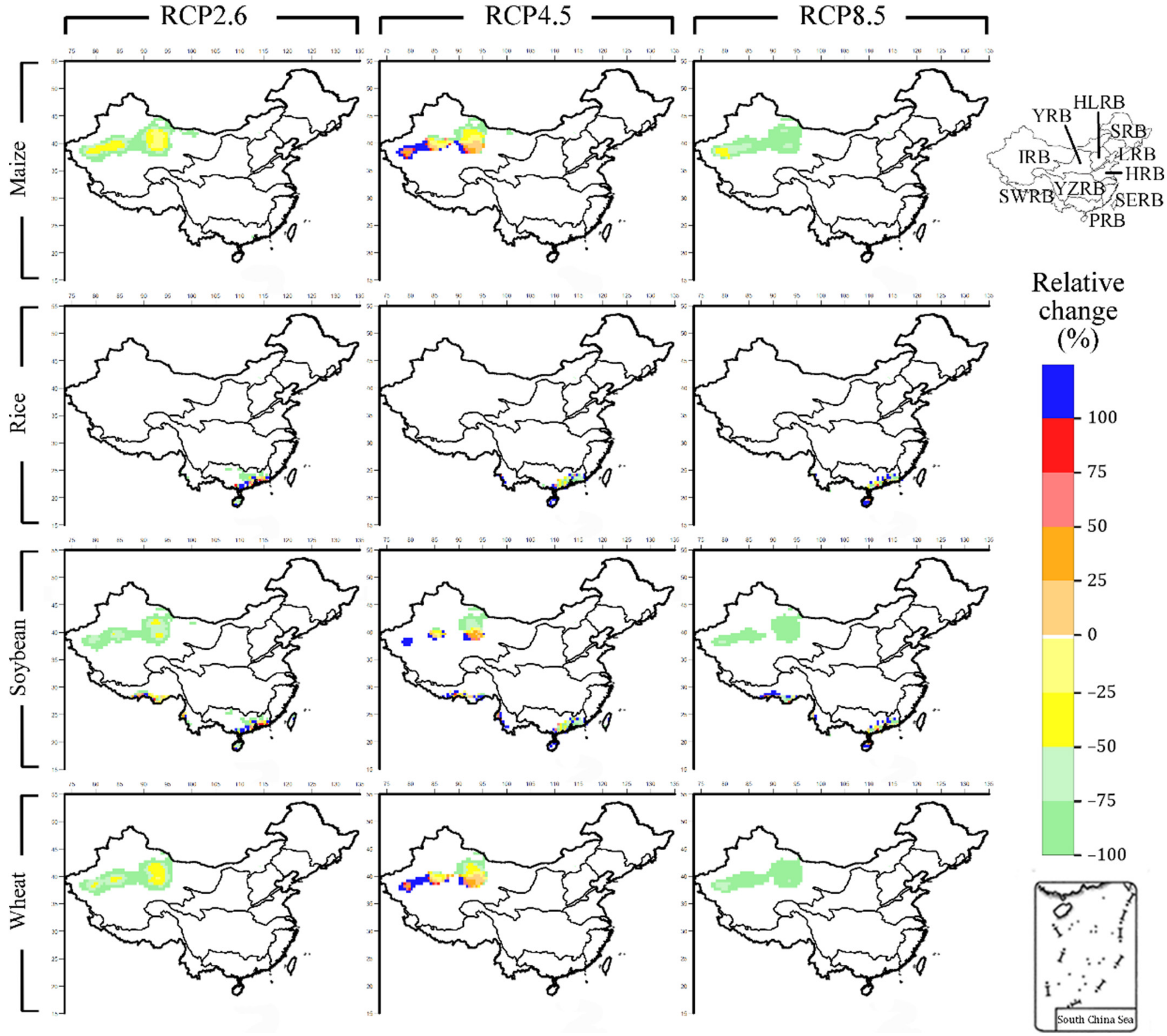

Fig. 2. Relative change (%) in the irrigation water requirement (IWR) for maize, rice, soybean and wheat by the end of this century (2090s; 2081–2100) compared with the baseline period (2006–2020) for the representative concentration pathway scenarios RCP2.6 (left-hand panels), RCP4.5 (center panels) and RCP8.5 (right-hand panels) at 0.5° resolution in China. Ten watershed regions in China are used: the Southwest Rivers Basin (SWRB), the Inland Rivers Basin (IRB), the Yellow River Basin (YRB), the Yangtze River Basin (YZRB), the Pearl River Basin (PRB), the Haihe and Luanhe Rivers Basin (HLRB), the Huaihe River Basin (HRB), the Southeast Rivers Basin (SERB), the Liaohe River Basin (LRB) and the Songhua River Basin (SRB).

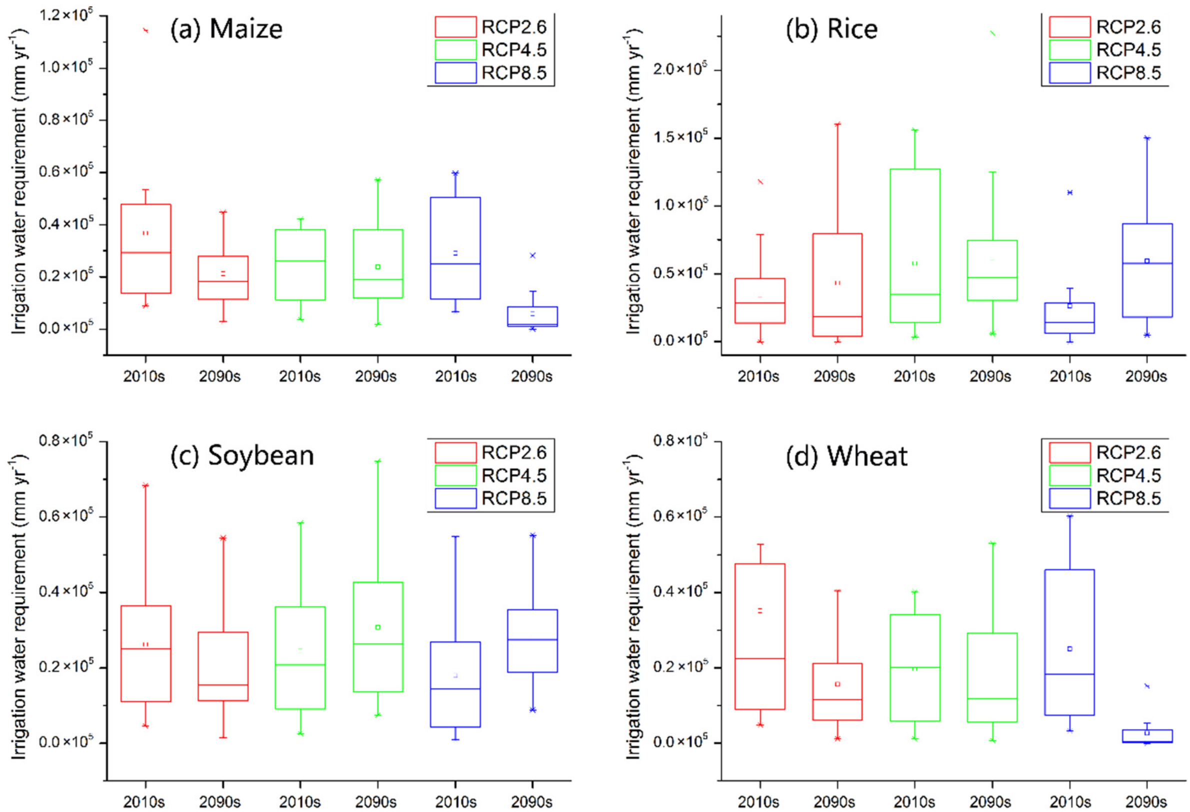

Fig. 3. Irrigation water requirements for (a) maize, (b) rice, (c) soybean and (d) wheat under the representative concentration pathway scenarios RCP2.6, RCP4.5 and RCP8.5 in China in the 2010s (2006–2020) and 2090s (2081–2100).

soil layer, and stored in the crop root zone for later use by the crops in transpiration. P_e is difficult to determine without detailed site-specific information. Here, P_e during the crop growth period can be simply approximated using Eq. (8), which is recommended by the FAO CROPWAT model (FAO, 2010):

$$P_e = \begin{cases} P \times \left(\dfrac{4.17-0.02 \times P}{4.17}\right), P<83\text{ mm} \\ 41.7 + 0.1 \times P, P \geq 83\text{ mm} \end{cases} \tag{8}$$

where P and P_e are the 10-day precipitation and effective precipitation, respectively, in millimeters.

2.3.4. Irrigation efficiency

The irrigation efficiency refers to the ratio of the net amount of water used by the crops to the total amount of water withdrawn from river channels or reservoirs. It includes water used in plant evapotranspiration, irrigation losses returned to the basin through runoff, seepage, infiltration, salt leaching and unproductive evaporation (Döll and Siebert, 2002; Wu and Zhou, 2011). The irrigation efficiency is not only affected by the crop type and variety, but also depends on the soil condition, irrigation method (e.g., drip, sprinkler, or surface irrigation) and the associated water conveyance efficiency (Fischer et al., 2007). Xiong et al. (2010) used irrigation water utilization coefficients of 0.6 for maize, wheat and soybean and 0.3 for rice to calculate the irrigation requirement. The value 0.3 for the irrigation water utilization coefficient for rice represents the amount of irrigation water used to maintain a certain depth of water in flooded fields during the growing season (Xiong et al., 2010). These coefficients are adopted in this study, allowed us to determine the optimum amount of water for each crop in each grid square under different climate change scenarios.

2.4. Data sources and processing

An ensemble of six high-resolution GCMs from the CMIP5 archive driven by multiple RCP scenarios was obtained from the Downscaled CMIP3 and CMIP5 Climate and Hydrology Projections (DCHP; https://gdo-dcp.ucllnl.org/downscaled_cmip_projections/dcpInterface.html#Projections:%20Complete%20Archives; last accessed Aug 2012) as scenarios of possible future climates to provide climate change forcing for our analysis (Maurer et al., 2007; Reclamation, 2013). Data from the DCHP were downscaled using the bias-correction and spatial disaggregation statistical technique (Wood et al., 2004). These six GCM model simulations, which appeared to perform well in simulating the spatial and temporal distribution of surface air temperature climatology and precipitation products, were used to calculate the multi-model ensemble mean with equal weight to improve performance in reproducing the observed changes in climate (Table 3) (e.g., Xu and Xu, 2012; Guo et al., 2013; Chen and Frauenfeld, 2014; Wang and Chen, 2014). Only the first ensemble member (denoted r1i1p1) from each model was considered. The CMIP5 models were forced by fixed atmospheric CO_2 mixing ratios under the RCPs. These annual mean mixing ratios up to 2100 are globally homogeneous and can be obtained from www.pik-potsdam.de/˜mmalte/rcps/ (last accessed May 2010) (Meinshausen et al., 2011).

The parameters obtained from the CMIP5 multi-model data were used to calculate the IWR (Zhang et al., 2017): the monthly mean maximum and minimum air temperatures were used to calculate ET_0 using the Penman–Monteith method. Based on ET_0 and K_c, the monthly precipitation was then used to calculate P_e and to obtain the IWR during different growth periods. To quantify the effects of temperature, precipitation and CO_2 concentrations on the IWR, we ran additional temperature-only (T-only), precipitation-only (P-only) and CO_2-only simulations in which the other two factors were retained at the 2006

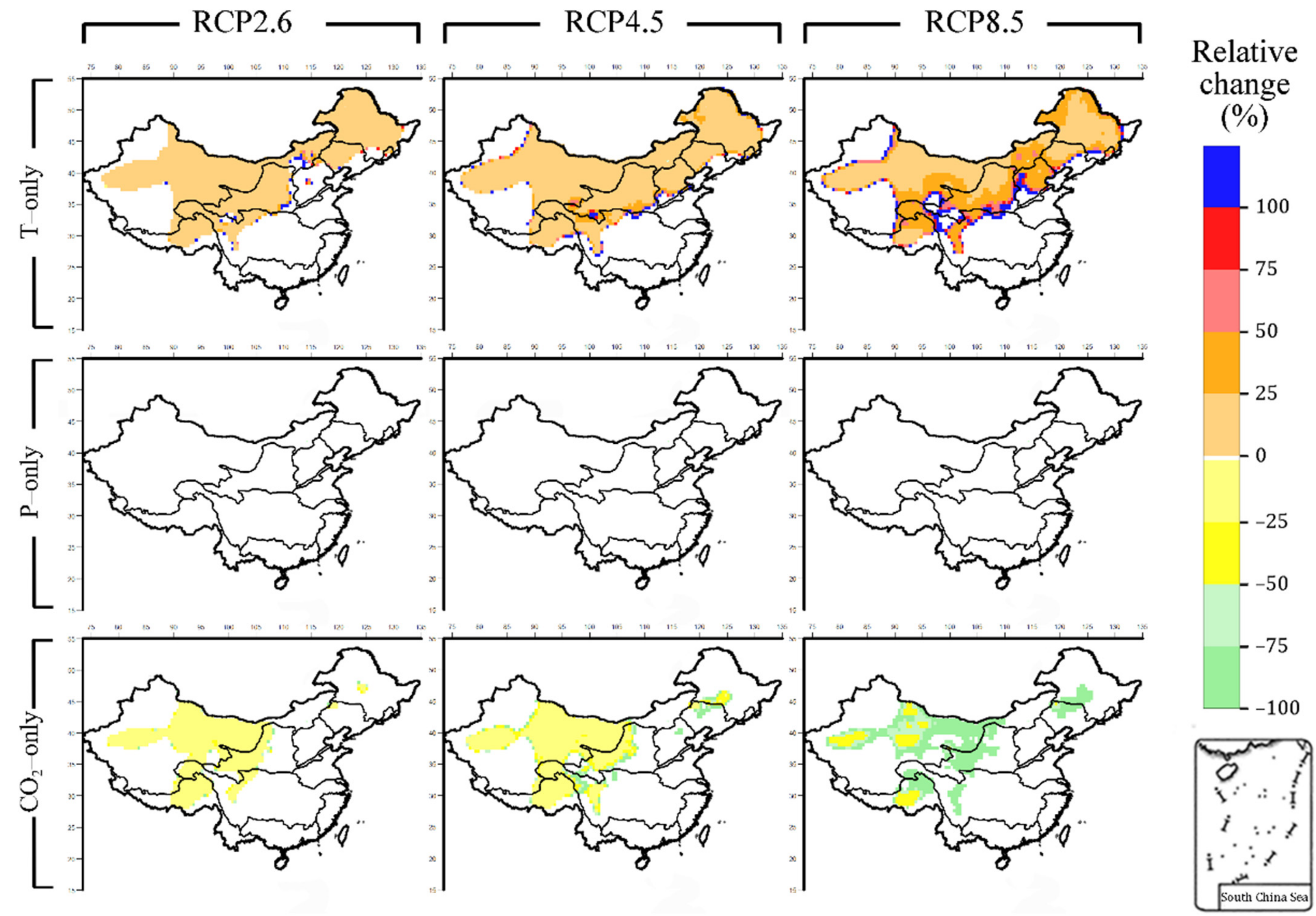

Fig. 4. Relative change (%) in the irrigation water requirement for maize by the end of this century (2090s; 2081–2100) compared with the baseline period (2006–2020) at 0.5° resolution in China. The results are shown with temperature-only (T-only), precipitation-only (P-only) and carbon dioxide-only (CO_2-only) scenarios for the representative concentration pathway scenarios RCP2.6, RCP4.5 and RCP8.5.

level. By comparing the differences in the changes between the T-only, P-only and CO_2-only scenarios, the sensitivity of the models to temperature, precipitation and atmospheric CO_2 concentrations when assessing the effects of climate change on the IWRs was investigated. The flow chart for the calculation under each RCP is shown in Fig. 1.

To facilitate comparison across spatial scales and time periods, ten watershed regions associated with major river basins in China were used: the Southwest Rivers Basin (SWRB), the Inland Rivers Basin (IRB), the Yellow River Basin (YRB), the Yangtze River Basin (YZRB), the Pearl River Basin (PRB), the Haihe and Luanhe Rivers Basin (HLRB), the Huaihe River Basin (HRB), the Southeast Rivers Basin (SERB), the Liaohe River Basin (LRB) and the Songhua River Basin (SRB) (Zhang et al., 2018a). The results of the different scenarios are presented as relative changes [(far future − baseline)/baseline]. The period between 2006 and 2020 (2010s) was chosen as the climate baseline for current conditions because these are the earliest years simulated by the RCP scenarios. The far future period (2090s; 2081–2100) was selected to highlight the impact of the largest possible variations in temperature, precipitation and CO_2 concentrations on irrigation at the end of the 21st century. It was more effective to use the same RCP datasets for method calibration and prediction.

This study was conducted without consideration of the coexistence of crops, although the growing season for maize is generally the same as that for rice in China. The proportions of areas (both rain-fed and irrigated) sown to crops in China were also neglected (paddy fields are all regarded as flooded rice fields). Moreover, the actual and potential distributions of crops were not considered during the calculation procedure using the climate-driven IWRs.

R (version 3.3.1; Statistics Department, University of Auckland, www.r-project.org/) was used to resample and clip all the datasets to the same spatial resolution of $0.5° \times 0.5°$ using bilinear interpolation. The datasets in the same spatial extent and time range were then applied to obtain the IWR during the crop growing season at the grid cell level. The R packages used in these calculation procedures were raster and ncdf4. R and Origin 8.5 (OriginLab Corporation, www.originlab.com/) were used to visualize the results.

3. Results

3.1. Relative changes in the IWR for different crops

For maize, the IWR decreased over a wide area of the IRB by the 2090s relative to the 2010s under the RCP2.6, RCP4.5 and RCP8.5 scenarios. The relative changes on the national scale were −42.40, −3.78 and −80.14%, respectively (Figs. 2 and 3). The decrease was larger under the RCP8.5 scenario, but a sharp increase also occurred in some western parts of the IRB under the RCP4.5 scenario.

For rice, the IWR showed large increases in the PRB by the 2090s relative to the 2010s under the RCP2.6, RCP4.5 and RCP8.5 scenarios. The relative changes on the national scale were 27.17, 6.12 and 126.34%,

respectively (Figs. 2 and 3). The increase in the IWR was larger under the RCP8.5 scenario.

For soybean, the IWR showed increases in the PRB and the south of the SWRB and decreases over a wide area of the IRB by the 2090s relative to the IWR in the 2010s under the RCP2.6, RCP4.5 and RCP8.5 scenarios. The relative changes on the national scale were −19.64, 25.11 and 57.23%, respectively (Figs. 2 and 3). A clear increase also occurred in some western parts of the IRB under the RCP4.5 scenario.

For wheat, the IWR decreased over a wide area of the IRB by the 2090s relative to the IWR in the 2010s under the RCP2.6, RCP4.5 and RCP8.5 scenarios. The relative changes on the national scale were −55.52, −11.68 and −89.32%, respectively (Figs. 2 and 3). The decrease was larger under the RCP8.5 scenario, although a clear increase also occurred in some western parts of the IRB under the RCP4.5 scenario.

3.2. Relative changes in the IWR for various climatic scenarios

Under the T-only scenario, increases in the IWR for maize were seen in almost all of northern and western China. The relative changes on the national scale were 2.44, 9.22 and 24.90% under the RCP2.6, RCP4.5 and RCP8.5 scenarios, respectively (Fig. 4). The area requiring irrigation was larger under the RCP4.5 scenario. The increasing trend was larger at the edges of the YRB under the RCP8.5 scenario. Under the CO_2-only scenario, decreases in the IWR for maize were seen in almost all of western China. The relative changes on the national scale were −3.58, −15.3 and −65.67% under the RCP2.6, RCP4.5 and RCP8.5 scenarios, respectively (Fig. 4). There was large decrease in the IWR in some eastern parts of western China under the RCP8.5 scenario. Under the P-only scenario, the IWR for maize implied zero growth.

Under the P-only scenario, increases in the IWR for rice were only seen in the PRB. The relative changes on the national scale were 35.72, 4.98 and 165.25% under the RCP2.6, RCP4.5 and RCP8.5 scenarios, respectively (Fig. 5). There were only minor spatial differences in the relative change in the IWR under the P-only scenario for rice and the increasing trend was larger under the RCP8.5 scenario. Under the T-only and CO_2-only scenarios, the IWR for rice implied zero growth, respectively.

Under the T-only scenario, increases in the IWR for soybean were seen in almost all of northern and western China. The relative changes on the national scale were 2.88, 9.57 and 25.91% under the RCP2.6, RCP4.5 and RCP8.5 scenarios, respectively (Fig. 6). The area requiring irrigation was larger under the RCP4.5 scenario. The increasing trend was larger in some regions of the YRB and HLRB under the RCP8.5 scenario. Under the P-only scenario, increases in the IWR for soybean were only seen in some scattered areas of the PRB and the south of the SWRB. The relative changes on a national scale were 26.76, 38.56 and 210.93% under the RCP2.6, RCP4.5 and RCP8.5 scenarios, respectively (Fig. 6). These spatial patterns were similar to the IWR for soybean and the increasing trend was larger under the RCP8.5 scenario. Under the CO_2-only scenario, decreases in the IWR for soybean were seen in almost all of western China. The relative changes on the national scale were −3.90, −15.75 and −64.01% under the RCP2.6, RCP4.5 and RCP8.5 scenarios, respectively

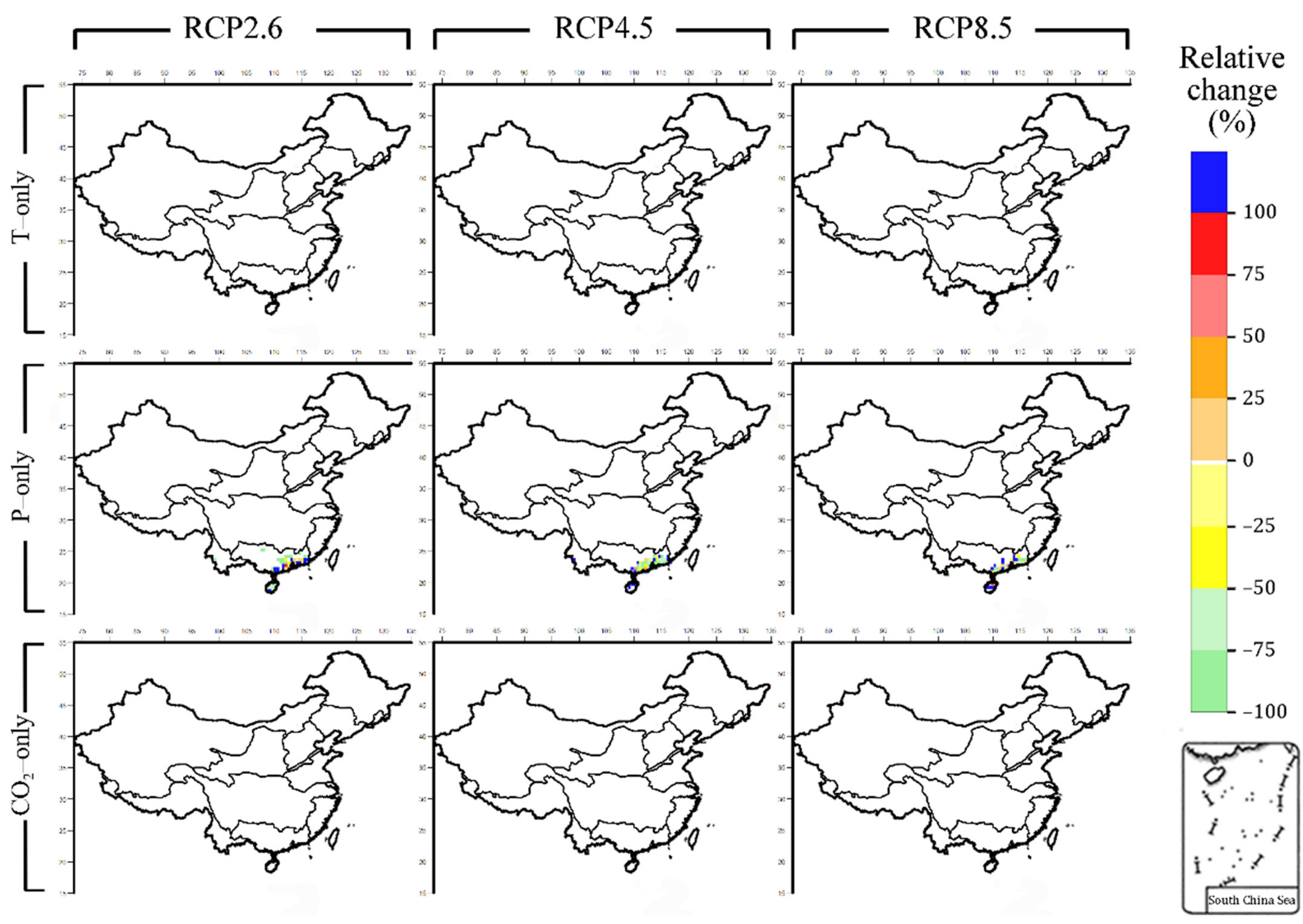

Fig. 5. Relative change (%) in the irrigation water requirement for rice by the end of this century (2090s; 2081–2100) compared with the baseline period (2006–2020) at 0.5° resolution in China. The results are shown with temperature-only (T-only), precipitation-only (P-only) and carbon dioxide-only (CO_2-only) scenarios for the representative concentration pathway scenarios RCP2.6, RCP4.5 and RCP8.5.

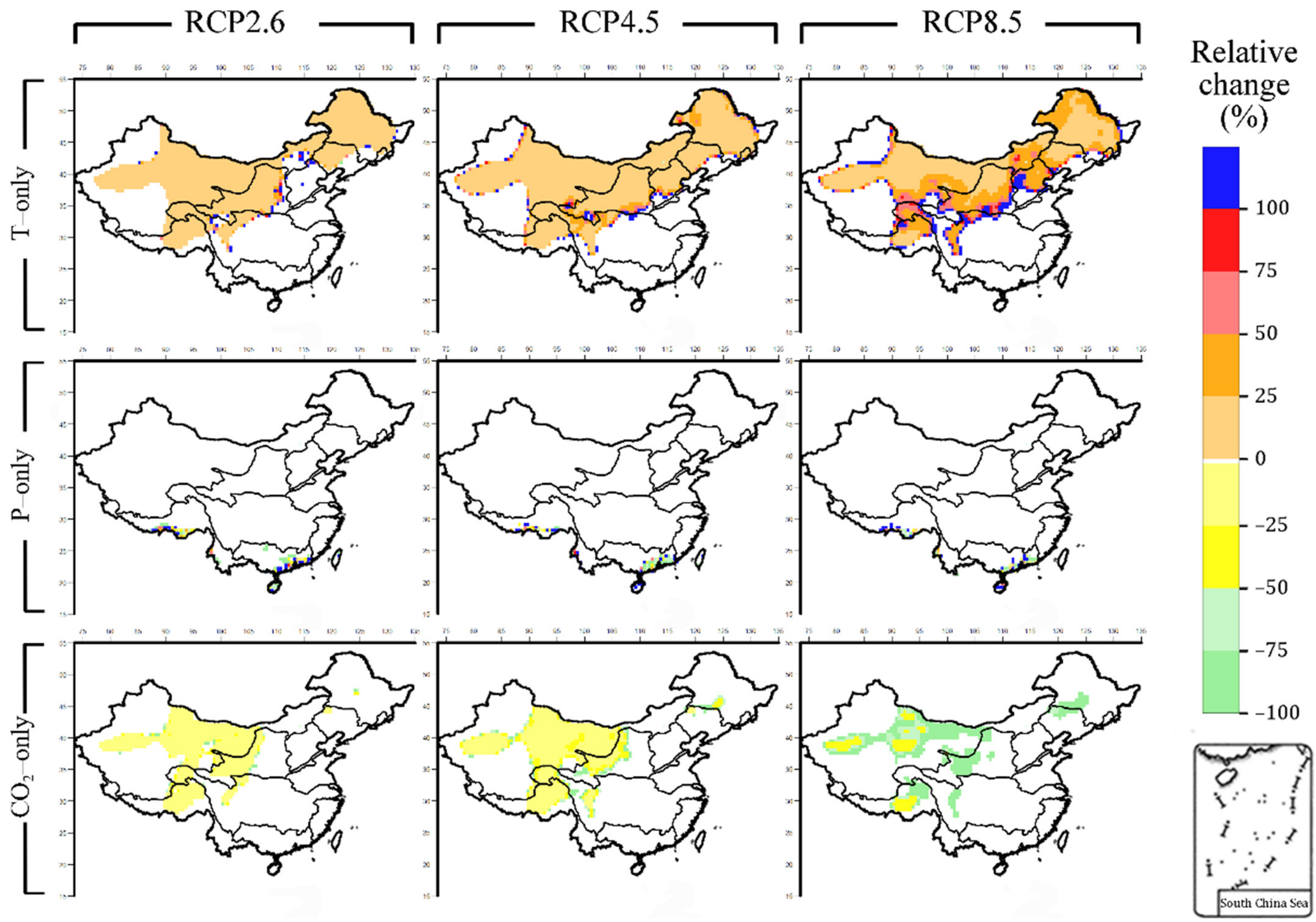

Fig. 6. Relative change (%) in the irrigation water requirement for soybean by the end of this century (2090s; 2081–2100) compared with the baseline period (2006–2020) at 0.5° resolution in China. The results are shown with temperature-only (T-only), precipitation-only (P-only) and carbon dioxide-only (CO_2-only) scenarios for the representative concentration pathway scenarios RCP2.6, RCP4.5 and RCP8.5.

(Fig. 6). A large decrease in the IWR was seen in some eastern parts of western China under the RCP8.5 scenario.

Under the T-only scenario, increases in the IWR for wheat were seen in almost all of northern and western China. The relative changes on the national scale were 2.68, 11.14 and 32.23% under the RCP2.6, RCP4.5 and RCP8.5 scenarios, respectively (Fig. 7). The area requiring irrigation was larger under the RCP4.5 scenario. The increasing trend was larger in northern and northeastern China and some eastern parts of western China under the RCP8.5 scenario. Under the CO_2-only scenario, decreases in the IWR for wheat were seen in almost all of western China and some parts of the SRB, LRB and HLRB. The relative changes on the national scale were −3.36, −15.27 and −67.03% under the RCP2.6, RCP4.5 and RCP8.5 scenarios, respectively (Fig. 7). A large decrease in the IWR occurred in the SRB and LRB and some eastern parts of western China under the RCP8.5 scenario. Under the P-only scenario, the IWR for wheat implied zero growth.

4. Discussion

4.1. Comparison with similar studies

As per Table 4, this study showed identical or similar results of spatial variations in the IWRs of crops compared with the results reported by Döll (2002), Cong et al. (2011) and Konzmann et al. (2013). This study effectively simulated the decreased IWRs of maize and wheat in IRB and the fluctuant IWR of rice in PRB. And our simulations were closest to the results reported by Konzmann et al. (2013), who quantified global changes in the irrigation requirements of major crop types using the Lund–Potsdam–Jena managed Land (LPJmL) model with climate projections from 19 GCMs up to the 2080s. Liu et al. (2009) reported the net irrigation water requirements for spring maize, summer maize, winter wheat and spring wheat for 1970–2000 were 400–800, 350–420, 300–500 and 300–550 mm yr^{-1} in Northwestern China, respectively; and the net irrigation water requirements for early, middle and late rice were 70–300, 90–250 and 100–450 mm yr^{-1} in Southern China, respectively. Cong et al. (2011) reported the net irrigation water requirements for maize and wheat for 2046–2065 under the SRES A1B scenario were 285.1 and 128.3 mm yr^{-1} in Northwestern China, respectively; and the net irrigation water requirement for rice was 286.6 mm yr^{-1} in Southern China. Compared with these studies, our simulations yielded different results mainly caused by the consideration of CO_2 effect and irrigation efficiency. Our findings were also generally consistent with the results of Zhu et al. (2015), which predicted the areas experiencing significant variations in irrigation requirements for three main crops (maize, rice and wheat) include Northwest China, Southeast China and Southwest China.

4.2. Relationship between climatic variables and variations in the IWR

The changes in climate during the 21st century in China described here (Fig. 8) include the following three aspects. (1) Warming is expected in most of regions of China under the RCP scenarios, with the

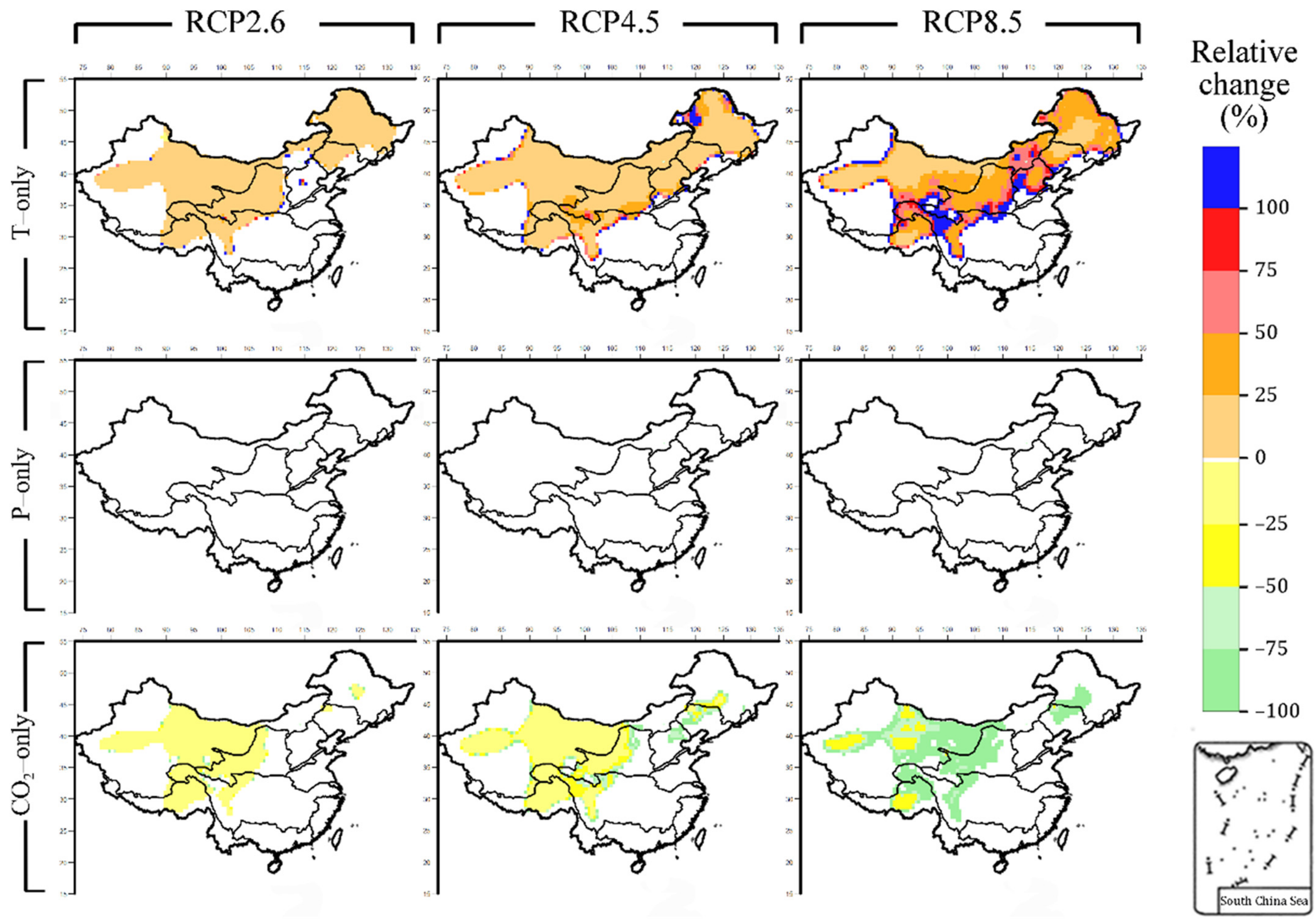

Fig. 7. Relative change (%) in the irrigation water requirement for wheat by the end of this century (2090s; 2081–2100) compared with the baseline period (2006–2020) at 0.5° resolution in China. The results are shown with temperature-only (T-only), precipitation-only (P-only) and carbon dioxide-only (CO_2-only) scenarios for the representative concentration pathway scenario RCP2.6, RCP4.5 and RCP8.5.

Qinghai–Tibetan Plateau showing greater warming than other regions and northern China showing slight cooling under the RCP2.6 scenario. Warming under the lower emission scenarios is less than under that under the higher emission scenarios. (2) The regional average precipitation will almost certainly increase (especially under the high-emission RCPs) and the increase in precipitation in the southern regions is clearer and greater than in the northern regions of China. And (3) the CO_2 concentration does not level off until 2100 under RCP8.5, whereas

Table 4
Estimated temporal and spatial variations in the irrigation water requirement for different crops in China. Ten watershed regions in China are used: the Southwest Rivers Basin (SWRB), the Inland Rivers Basin (IRB), the Yellow River Basin (YRB), the Yangtze River Basin (YZRB), the Pearl River Basin (PRB), the Haihe and Luanhe Rivers Basin (HLRB), the Huaihe River Basin (HRB), the Southeast Rivers Basin (SERB), the Liaohe River Basin (LRB) and the Songhua River Basin (SRB). GCM, global climate model; SRES, Special Report on Emission Scenarios; RCP, representative concentration pathway.

Remark	Method	Data source	Carbon dioxide effect	Time period	Crop type	Spatial variation trend of irrigation water requirement in regions of China (“↑” means increase; “↓” means decrease; and “→” means steady)									
						SWRB	IRB	YRB	YZRB	PRB	HLRB	HRB	SERB	LRB	SRB
Döll (2002)	WaterGAP model and crop coefficient method	ECHAM4 and HadCM3	Without consideration	1961–1990 2020–2029	Rice and non-rice	→	↑	↑/↓	→	↑	↑	↓	→	↑/↓	↑
Cong et al. (2011)	FAO Penman–Monteith equation and crop coefficient method	MIROC3.2 under SRES A1B and 20C3M scenarios	Without consideration	1961–1990 2046–2065	Maize	→	↓	↑/↓	↓	↑	↑	↓	→	↑	→
					Rice	→	↓	↓	↓	↑/↓	↑	↓	→	↑	↑
					Wheat	↑	↓	↓	↑/↓	↑	↓	↓	↑	↑/↓	↑
Konzmann et al. (2013)	LPJmL model	CRU TS3.0 and 19 GCMs under SRES A2 scenario	With consideration	1971–2000 2070–2099	12 crop types [including maize, rice, soybean and temperate cereals (wheat, barley, rye)]	↑	↑	↑/↓	↓	↑	↑	↓	↓	↓	↓
This study	FAO Penman–Monteith equation and crop coefficient method	6 GCMs under 3 RCP scenarios (take RCP8.5 for example)	With consideration	2006–2020 2081–2100	Maize		↓								
					Rice					↑/↓					
					Soybean	↑/↓	↓			↑/↓					
					Wheat		↓								

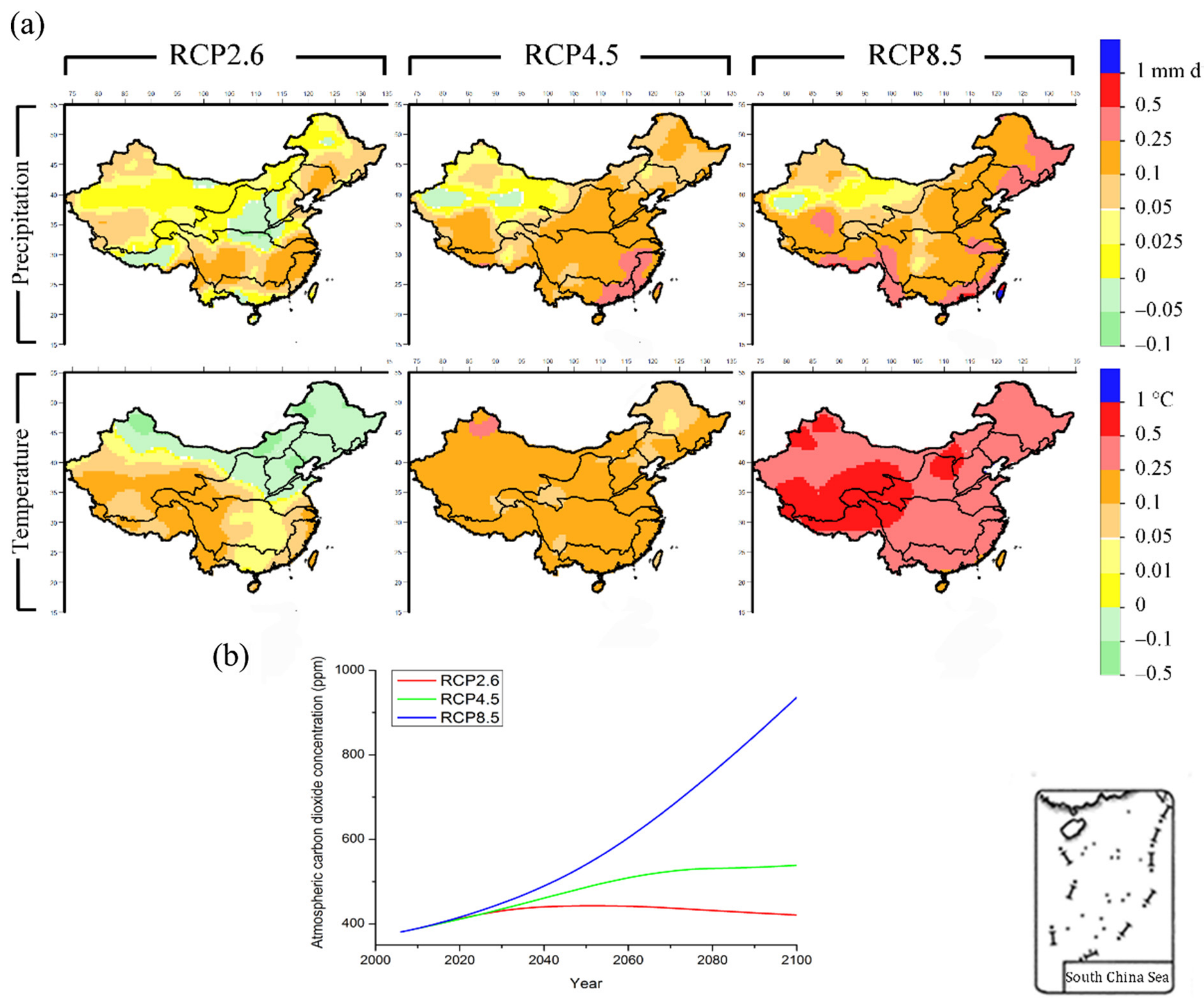

Fig. 8. Changes in the climatic variables of precipitation, temperature and carbon dioxide concentrations for the representative concentration pathway scenarios RCP2.6, RCP4.5 and RCP8.5 in China. The results are shown for (a) the differences in precipitation and temperature between the end of this century (2090s; 2081–2100) and the baseline period (2006–2020) at 0.5° resolution, and (b) the trend in globally homogeneous atmospheric carbon dioxide concentrations from 2006 to 2100.

the CO_2 level under RCP4.5 stabilizes by the mid-2100s and there is an ongoing slow decrease in CO_2 concentrations from the mid-2100s under RCP2.6. These results agree with previous research (e.g., Xu and Xu, 2012; Zhao et al., 2014).

Previous research has shown that climate change—with global changes in temperature, precipitation and atmospheric CO_2 concentrations—is likely to be the dominant factor governing temporal and spatial changes in the IWR (Döll, 2002; Zhang et al., 2012; Leng and Tang, 2014). The increase in temperature may increase photorespiration in crops by changing the kinetics and activity of enzyme, further reduce crop water use efficiency (or the ratio of yield to transpiration) and increase the IWR; the decrease in precipitation may directly cause an upward trend in the IWR (Cong et al., 2011; Winter et al., 2017). In addition, increasing atmospheric concentrations of CO_2 may cause a reduction in stomatal conductance and affect crop transpiration (Islam et al., 2012; Deryng et al., 2016). These factors will contribute to improving the efficiency of water use by crops and will mitigate the IWR (Döll, 2002; Ficklin et al., 2010; Pan et al., 2015). However, except for rice, the variations of IWR for other crops are not determined by any single climatic factor in this study (as per Figs. 4, 5, 6 and 7). As a result of the combination of increasing temperatures, regional increases in precipitation and the beneficial effects of increased CO_2 on plants, the amount of irrigation required for most of crops in China may be alleviated under the high-emission RCPs (Turral et al., 2010; Konzmann et al., 2013; Leng and Tang, 2014).

Under the RCP8.5 scenario, the variations in the IWRs of maize and wheat are affected by the temperature and CO_2 concentrations and show a decrease over time caused by the effects of CO_2 on the IWR offsetting the effect of increasing temperatures (Figs. 9 and 10). By contrast, the IWR for soybean shows an increasing trend under the co-action of climatic variables especially in the PRB and SWRB (Figs. 9 and 10). For rice crops, the amount of precipitation is the main effect on the variations in the IWR because higher levels of irrigation are required by rice than other crops and may partly protect rice from the negative effects of increased temperatures (Figs. 9 and 10) (Hatfield et al., 2011; Gourdji et al., 2013). In the arid inland regions, the IWRs of maize and wheat are more sensitive to crop evapotranspiration, which can be estimated from the data on temperature and CO_2 concentrations, as a result of low rainfall and high rates of evaporation (Shen et al., 2013). Annual precipitation is generally <50 mm in the oasis areas, where most agricultural activities exist (Shen et al., 2013). However, the opposite effect is seen for rice in the southern coastal regions, where the variation of precipitation dominates hydroclimatic conditions (Zhang and Sun, 2012). These results agree with those of Konzmann et al. (2013). This is because the inland region of northwestern China is controlled by a continental climate, with little rainfall throughout the year and strong evaporative potential. The mean annual precipitation is only 130 mm, with uneven spatial and temporal distributions, and the potential evaporation can be as large as

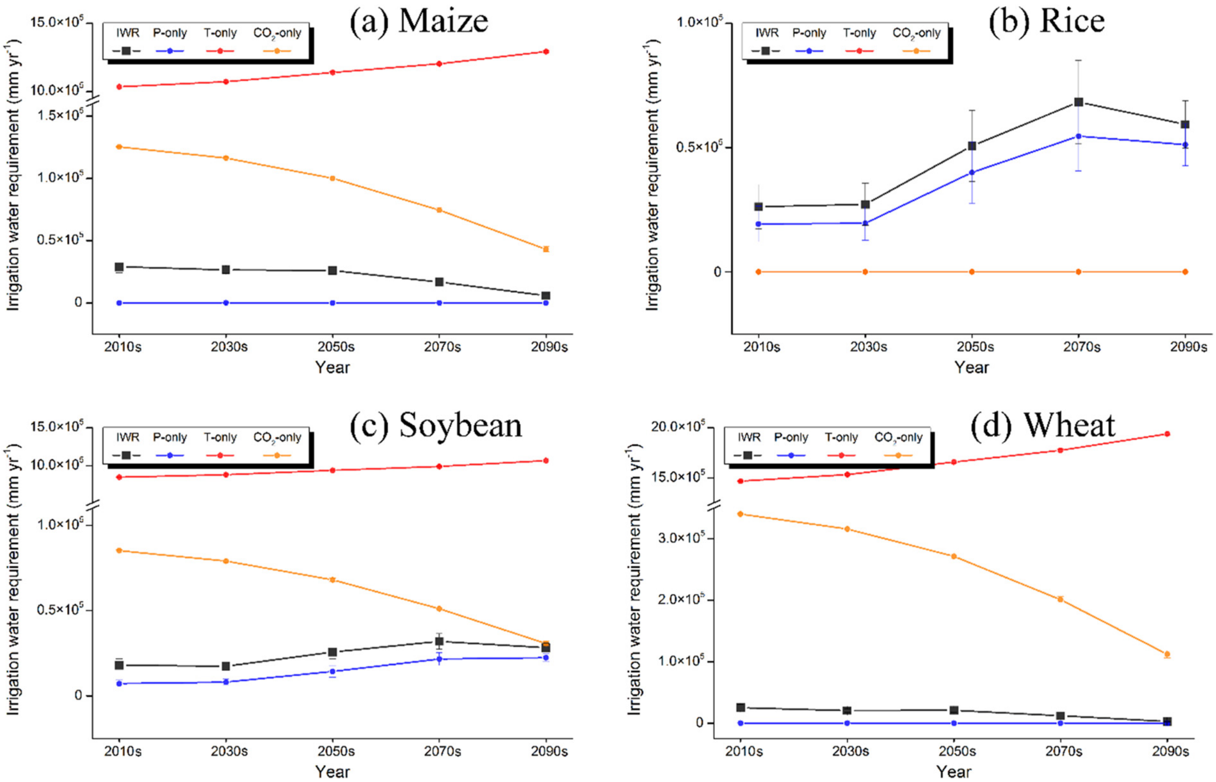

Fig. 9. Irrigation water requirements (calculated as: mean ± 1 SE) with temperature-only (T-only), precipitation-only (P-only) and carbon dioxide-only (CO_2-only) scenarios for (a) maize, (b) rice, (c) soybean and (d) wheat under the representative concentration pathway scenario RCP8.5 in China in the 2010s (2006–2020), 2030s (2021–2040), 2050s (2041–2060), 2070s (2061–2080) and 2090s (2081–2100).

3200 mm yr^{-1}. The demand for irrigation water in this highly water-deficient region is therefore an important consideration in the allocation of water resources (Shen et al., 2013). The southern coastal region has the large area of irrigated crops, the high intensity of irrigation and the highest intensity of crops (Amarasinghe et al., 2005). The development of agriculture in these regions relies entirely on irrigation (Tao et al., 2003; Liu et al., 2009).

4.3. Limitations of this study

Like most studies on the effects of climate change on agricultural irrigation, there are several limitations associated with this study. Future research should aim to develop a high spatiotemporal resolution dataset and a better irrigation module to eliminate these limitations.

1. Climate variability accounts for most of the variability in the amount of irrigation required by crops in most regions. However, the lack of consideration of other socioeconomic and environmental factors affecting the IWRs of crops may result in discrepancies in our results. The newly developed shared socioeconomic pathways method may help to assess irrigation requirements taking into account the joint pressures from climate change and socioeconomic development (Yin et al., 2017).
2. The approach used in this study does not fully reflect regional fertilization and irrigation practices in which farmers may adapt to changing weather patterns to reduce the peak demands for irrigation, leading to different crop calendars (Wada et al., 2013). Irrigation was not considered when rainfall fulfilled the requirements for crop growth in this study, which may underestimate the amount of irrigation water actually required.
3. Climate variability also affects crop growth, not only ET_0; different leaf area indexes can result in different values of K_c. In addition, the irrigation efficiency is determined by the condition of the irrigation canal, the soil type and the level of irrigation management. These factors differ for the same crop in different regions of China due to differences in financial investments by local governments and the current level of development of irrigation systems (Zhu et al., 2015). The approach used in this study considered the crop coefficient and irrigation efficiency as fixed values for four crop types under different climate change scenarios, which may have led to inaccuracies in the calculation of the IWR. Gridded maps of irrigation efficiencies are available—with direct linkages to differences in the type of agricultural system and crops, the climatic and hydrological conditions and overall crop management—but they apply to fixed extents of croplands and areas equipped for irrigation (e.g., Jägermeyr et al., 2015). Further study is needed to estimate crop coefficient and irrigation efficiency associated with future changes in climate variables and land use (Wada et al., 2014).
4. This study assumed that the effective rainfall available for crops did not include the precipitation intercepted by the plant canopy, surface runoff and water percolating to below the root zone. The implication of this assumption may overestimate the amount of water available from precipitation and therefore underestimate the IWR (Turral et al., 2010). In addition, this study assumed the soil water storage, capillary rise and leaching requirement to be zero. Considering the water balance in the root zone of irrigated soil, the capillary rise and the decreased soil water storage and leaching requirement may lead to lower IWR (Beltrán, 1999).
5. The effect of CO_2 on the IWR of different crops was assumed to be the same. However, some research has suggested that higher atmospheric CO_2 concentrations reduce water loss and the use of water by C3 crops (e.g., rice, soybean and wheat), whereas C4 crops do not show changes in water use efficiency with higher temperatures and increased atmospheric CO_2 concentrations (e.g., Winter et al., 2017). Furthermore, the reductions in stomatal conductance (g) under elevated CO_2 level are different for C3 and C4 crops, which

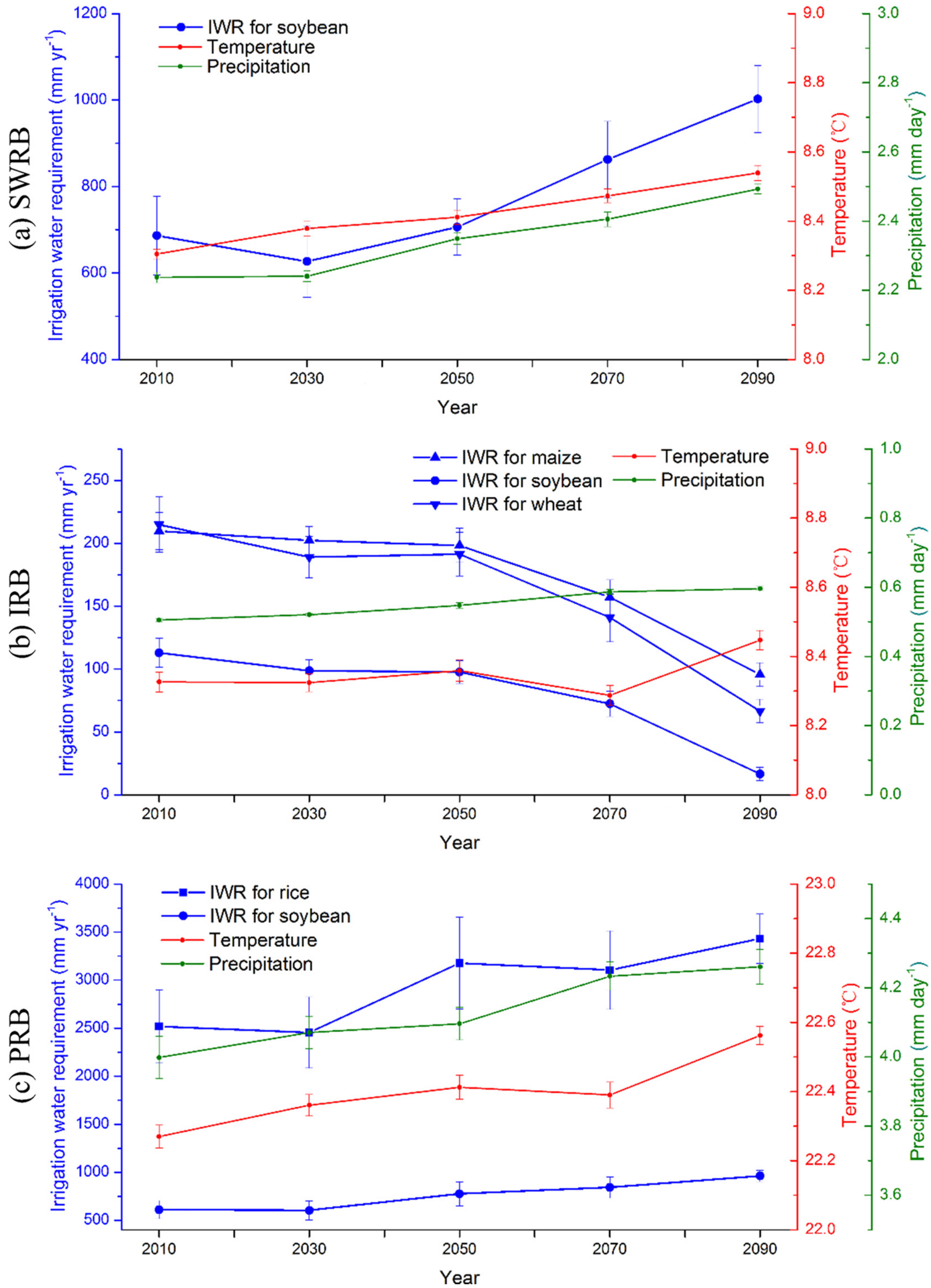

Fig. 10. Changes in temperature, precipitation and irrigation water requirements (IWR; calculated as: mean ± 1 SE) for maize, rice, soybean and wheat under the representative concentration pathway scenario RCP8.5 in three watershed regions [(a) the Southwest Rivers Basin (SWRB), (b) the Inland Rivers Basin (IRB) and (c) the Pearl River Basin (PRB)] in China in the 2010s (2006–2020), 2030s (2021–2040), 2050s (2041–2060), 2070s (2061–2080) and 2090s (2081–2100).

need to be further adjusted and corrected by some reported relationships (Islam et al., 2012).

6. This study assumed that the growing season of crops would be unaffected by climate change. However, crops grown under increasing temperatures and higher CO_2 concentrations may have shorter growing periods and different sowing dates, which would affect the irrigation scheme and requirement (Turral et al., 2010).

5. Conclusions and perspective

This study investigated the effects of future climate change on the IWRs of maize, rice, soybean and wheat in China using the FAO Penman–Monteith equation (incorporating the CO_2 effect) and the crop coefficient approach. Substantially different spatiotemporal patterns of the IWR were derived under different RCP scenarios due to the combination of increasing temperatures, regional increases in

precipitation and the beneficial effects of CO_2 on plants. The regions that will require irrigation water as a result of climate change are widely distributed in northwestern China for all crops except for rice, and in southern and southwestern China for both rice and soybean crops. Moreover, the IWRs for crops may decrease gradually over time in China, especially under the RCP8.5 scenario, mainly due to increasing concentrations of CO_2. This does not imply that water scarcity in agriculture will be alleviated in the future. Under increasing temperatures and higher CO_2 concentrations, crops grown may have lower quality and lower nutrient composition, which would increase the amount of water needed to produce the required number of calories (Gerten et al., 2011). Irrigated agriculture in China still faces challenges under the predicted changes in climate. Improved water-saving measures (such as better maintenance of the irrigation infrastructure and adaptation of more advanced irrigation technology) are required in agriculture to compensate for the increases in irrigation requirements due to agricultural development, and to meet the urgent need for the rational use and protection of water resources.

Overall, the method used in this study achieved effective simulation results with a lower data requirement (mainly on geography and air temperatures), a simpler calculation procedure than in previous studies and with consideration of the effects of changes in atmospheric CO_2 concentrations on the IWR for crops. Although some sorts of limitations exist in this method, it is worth further developing and applying in the simulation of IWR for crops under limited data condition. It is crucial in developing integrated irrigation models, and designing adaptation strategies for food supply and the sustainable development of agriculture under a climate change regime.

Acknowledgments

The authors are indebted to Jing Ge and Gaopeng Li at the Shanghai Institutes for Biological Sciences, Chinese Academy of Sciences, Shanghai, and Yao Li at the College of Resources and Environment, University of Chinese Academy of Sciences, Beijing, for their suggestions. The authors are also grateful to the anonymous referees and the handling editor for the provision of constructive and useful reviews and advice that have led to a substantially improved revised paper. This study was funded through the National Key Research and Development Program of China (Grant No. 2016YFC0501803).

References

Allen, R.G., Pereira, L.S., Raes, D., Smith, M., 1998. Crop evapotranspiration: guidelines for computing crop requirements. FAO Irrigation and Drainage Paper No. 56, p. 300 Rome, Italy.

Almorox, J., Senatore, A., Quej, V.H., Mendicino, G., 2018. Worldwide assessment of the Penman–Monteith temperature approach for the estimation of monthly reference evapotranspiration. Theor. Appl. Climatol. 131, 693–703.

Amarasinghe, U.A., Giordano, M., Liao, Y.S., Shu, Z.P., 2005. Water supply, water demand and agricultural water scarcity in China: a basin approach. Country Policy Support Program Report 11. International Commission on Irrigation and Drainage, New Delhi.

Beltrán, J., 1999. Irrigation with saline water: benefits and environmental impact. Agric. Water Manag. 40, 183–194.

Bortolini, L., Maucieri, C., Borin, M., 2018. A tool for the evaluation of irrigation water quality in the arid and semi-arid regions. Agronomy 8, 23. https://doi.org/10.3390/agronomy8020023.

Chen, L., Frauenfeld, O., 2014. A comprehensive evaluation of precipitation simulations over China based on CMIP5 multimodel ensemble projections. J. Geophys. Res. Atmos. 119, 5767–5786.

Cong, Z.T., Yao, B.Z., Ni, G.H., 2011. Crop water demand in China under the SRA1B emissions scenario. Adv. Water Sci. 22, 38–43.

Dam, J., Malik, R., 2003. Water Productivity of Irrigated Crops in Sirsa District, India; Integration of Remote Sensing, Crop and Soil Models and Geographical Information Systems. Wageningen Universiteit, Wageningen.

Deryng, D., Elliott, J., Folberth, C., Müller, C., Pugh, T., Boote, K., Conway, D., Ruane, A., Gerten, D., Jones, J., Khabarov, N., Olin, S., Schaphoff, S., Schmid, E., Yang, H., Rosenzweig, C., 2016. Regional disparities in the beneficial effects of rising CO_2 concentrations on crop water productivity. Nat. Clim. Chang. 6, 786–790.

Döll, P., 2002. Impact of climate change and variability on irrigation requirements: a global perspective. Clim. Chang. 54, 269–293.

Döll, P., Siebert, S., 2002. Global modeling of irrigation water requirements. Water Resour. Res. 38, 1037. https://doi.org/10.1029/2001WR000355.

Elliott, J., Deryng, D., Müller, C., Frieler, K., Konzmann, M., Gerten, D., Glotter, M., Flörke, M., Wada, Y., Best, N., Eisner, S., Fekete, B.M., Folberth, C., Foster, I., Gosling, S.N., Haddeland, I., Khabarov, N., Ludwig, F., Masaki, Y., Olin, S., Rosenzweig, C., Ruane, A.C., Satoh, Y., Schmid, E., Stacke, T., Tang, Q., Wisser, D., 2014. Constraints and potentials of future irrigation water availability on agricultural production under climate change. Proc. Natl. Acad. Sci. U. S. A. 111, 3239–3244.

Fang, Q.X., Ma, L., Green, T.R., Yu, Q., Wang, T.D., Ahuja, L.R., 2010. Water resources and water use efficiency in the North China Plain: current status and agronomic management options. Agric. Water Manag. 97, 1102–1116.

Fares, A., Awal, R., Fares, S., Johnson, A., Valenzuela, H., 2016. Irrigation water requirements for seed corn and coffee under potential climate change scenarios. J. Water Clim. Chang. 7, 39–51.

Ficklin, D., Luedeling, E., Zhang, M., 2010. Sensitivity of groundwater recharge under irrigated agriculture to changes in climate, CO_2 concentrations and canopy structure. Agric. Water Manag. 97, 1039–1050.

Fischer, G., Tubiello, F.N., van Velthuizen, H., Wiberg, D.A., 2007. Climate change impacts on irrigation water requirements: effects of mitigation, 1990–2080. Technol. Forecast. Soc. Chang. 74, 1083–1107.

Food and Agriculture Organization of the United Nations, 2010. Land and Water Development Division. CROPWAT Model. FAO, Rome, Italy.

Gerten, D., Schaphoff, S., Lucht, W., 2007. Potential future changes in water limitation of the terrestrial biosphere. Clim. Chang. 80, 277–299.

Gerten, D., Heinke, J., Hoff, H., Biemans, H., Fader, M., Waha, K., 2011. Global water availability and requirements for future food production. J. Hydrometeorol. 12, 885–899.

Gourdji, S., Sibley, A., Lobell, D., 2013. Global crop exposure to critical high temperatures in the reproductive period: historical trends and future projections. Environ. Res. Lett. 8, 024041. https://doi.org/10.1088/1748-9326/8/2/024041.

Guo, Y., Dong, W.J., Ren, F.M., Zhao, Z.C., Huang, J.B., 2013. Surface air temperature simulations over China with CMIP5 and CMIP3. Adv. Clim. Chang. Res. 4, 145–152.

Hatfield, J.L., Boote, K.J., Kimball, B.A., Ziska, L.H., Izaurralde, R.C., Ort, D., Thomson, A.M., Wolfe, D., 2011. Climate impacts on agriculture: implications for crop production. Agron. J. 103, 351–370.

Islam, A., Ahuja, L., Garcia, L., Ma, L., Saseendran, A., 2012. Modeling the effect of elevated CO_2 and climate change on reference evapotranspiration in the Semi-arid Central Great Plains. Trans. ASABE 55, 2135–2146.

Jägermeyr, J., Gerten, D., Heinke, J., Schaphoff, S., Kummu, M., Lucht, W., 2015. Water savings potentials of irrigation systems: global simulation of processes and linkages. Hydrol. Earth Syst. Sci. 19, 3073–3091.

Konzmann, M., Gerten, D., Heinke, J., 2013. Climate impacts on global irrigation requirements under 19 GCMs, simulated with a vegetation and hydrology model. Hydrol. Sci. J. 58, 88–105.

Leff, B., Ramankutty, N., Foley, J., 2004. Geographic distribution of major crops across the world. Glob. Biogeochem. Cycles 18, GB1009. https://doi.org/10.1029/2003GB002108.

Leng, G.Y., Tang, Q.H., 2014. Modeling the impacts of future climate change on irrigation over China: sensitivity to adjusted projections. J. Hydrometeorol. 15, 2085–2103.

Liu, Y., Pereira, L.S., 2000. Validation of FAO methods for estimating crop coefficients. Trans. Chin. Soc. Agric. Eng. 16, 26–30.

Liu, Y., Wang, L., Ni, G.H., Cong, Z.T., 2009. Spatial distribution characteristics of irrigation water requirement for main crops in China. Trans. Chin. Soc. Agric. Eng. 25, 6–12.

Maurer, E.P., Brekke, L., Pruitt, T., Duffy, P.B., 2007. Fine-resolution climate projections enhance regional climate change impact studies. EOS Trans. Am. Geophys. Union 88, 504.

Meinshausen, M., Smith, S., Calvin, K., Daniel, J., Kainuma, M., Lamarque, J.-F., Matsumoto, K., Montzka, S., Raper, S., Riahi, K., Thomson, A., Velders, G., van Vuuren, D., 2011. The RCP greenhouse gas concentrations and their extension from 1765 to 2500. Clim. Chang. 109, 213–241.

Moss, R., Edmonds, J., Hibbard, K., Manning, M., Rose, S., van Vuuren, D., Carter, T., Emori, S., Kainuma, M., Kram, T., Meehl, G., Mitchell, J., Nakicenovic, N., Riahi, K., Smith, S., Stouffer, R., Thomson, A., Weyant, J., Wilbanks, T., 2010. The next generation of scenarios for climate change research and assessment. Nature 463, 747–756.

Pan, S., Tian, H., Dangal, S., Yang, Q., Yang, J., Lu, C., Tao, B., Ren, W., Ouyang, Z., 2015. Responses of global terrestrial evapotranspiration to climate change and increasing atmospheric CO_2 in the 21st century. Earth Future 3, 15–35.

Pandey, P.K., Pandey, V., 2016. Evaluation of temperature-based Penman–Monteith (TPM) model under the humid environment. Model. Earth Syst. Environ. 2, 152. https://doi.org/10.1007/s40808-016-0204-9.

Pfister, S., Bayer, P., Koehler, A., Hellweg, S., 2011. Projected water consumption in future global agriculture: scenarios and related impacts. Sci. Total Environ. 409, 4206–4216.

Raziei, T., Pereira, L., 2013. Estimation of ET_0 with Hargreaves-Samani and FAO-PM temperature methods for a wide range of climates in Iran. Agric. Water Manag. 121, 1–18.

Reclamation, 2013. Downscaled CMIP3 and CMIP5 Climate and Hydrology Projections: Release of Downscaled CMIP5 Climate Projections, Comparison With Preceding Information, and Summary of User Needs. (Prepared by the U.S. Department of the Interior, Bureau of Reclamation, Technical Services Center, Denver, Colorado). p. 47.

Sacks, W.J., Deryng, D., Foley, J.A., Ramankutty, N., 2010. Crop planting dates: an analysis of global patterns. Glob. Ecol. Biogeogr. 19, 607–620.

Shen, Y.J., Li, S., Chen, Y.N., Qi, Y.Q., Zhang, S.W., 2013. Estimation of regional irrigation water requirement and water supply risk in the arid region of Northwestern China 1989–2010. Agric. Water Manag. 128, 55–64.

Stockle, C., Williams, J., Rosenberg, N., Jones, C., 1992. A method for estimating the direct and climatic effects of rising atmospheric carbon dioxide on growth and yield of crops: part 1. Modification of the EPIC model for climate change analysis. Agric. Syst. 38, 225–238.

Tao, F.L., Yokozawa, M., Hayashi, Y., Lin, E.D., 2003. Future climate change, the agricultural water cycle, and agricultural production in China. Agric. Ecosyst. Environ. 95, 203–215.
Taylor, K.E., Stouffer, R.J., Meehl, G.A., 2012. An overview of CMIP5 and the experiment design. Bull. Am. Meteorol. Soc. 93, 485–498.
Thomas, A., 2008. Agricultural irrigation demand under present and future climate scenarios in China. Glob. Planet. Chang. 60, 306–326.
Turral, H., Svendsen, M., Faures, J.M., 2010. Investing in irrigation: reviewing the past and looking to the future. Agric. Water Manag. 97, 551–560.
van Vuuren, D., Edmonds, J., Kainuma, M., Riahi, K., Thomson, A., Hibbard, K., Hurtt, G., Kram, T., Krey, V., Lamarque, J., Masui, T., Meinshausen, M., Nakicenovic, N., Smith, S., Rose, S., 2011. The representative concentration pathways: an overview. Clim. Chang. 109, 5–31.
Wada, Y., Wisser, D., Eisner, S., Flörke, M., Gerten, D., Haddeland, I., Hanasaki, N., Masaki, Y., Portmann, F.T., Stacke, T., Tessler, Z., Schewe, J., 2013. Multimodel projections and uncertainties of irrigation water demand under climate change. Geophys. Res. Lett. 40, 4626–4632.
Wada, Y., Wisser, D., Bierkens, M.F.P., 2014. Global modeling of withdrawal, allocation and consumptive use of surface water and groundwater resources. Earth Syst. Dyn. 5, 15–40.
Wang, L., Chen, W., 2014. A CMIP5 multimodel projection of future temperature, precipitation, and climatological drought in China. Int. J. Climatol. 34, 2059–2078.
Wang, W.G., Yu, Z.B., Zhang, W., Shao, Q.X., Zhang, Y.W., Luo, Y.F., Jiao, X.Y., Xu, J.Z., 2014. Responses of rice yield, irrigation water requirement and water use efficiency to climate change in China: historical simulation and future projections. Agric. Water Manag. 146, 249–261.
Wang, J.Q., Liu, X.Y., Cheng, K., Zhang, X.H., Li, L.Q., Pan, G.X., 2018. Winter wheat water requirement and utilization efficiency under simulated climate change conditions: a Penman–Monteith model evaluation. Agric. Water Manag. 197, 100–109.
Winter, J.M., Lopez, J.R., Ruane, A.C., Young, C.A., Scanlon, B.R., Rosenzweig, C., 2017. Representing water scarcity in future agricultural assessments. Anthropocene 18, 15–26.
Wood, A.W., Leung, L.R., Sridhar, V., Lettenmaier, D.P., 2004. Hydrologic implications of dynamical and statistical approaches to downscaling climate model outputs. Clim. Chang. 62, 189–216.
Wu, X., Zhou, H., 2011. Influence factor to water transport index in canal system in Xinjiang irrigation area. Yellow River 9, 93–97.
Xiong, W., Conway, D., Lin, E.D., Xu, Y.L., Ju, H., Jiang, J.H., Holman, I., Li, Y., 2009. Future cereal production in China: the interaction of climate change, water availability and socio-economic scenarios. Glob. Environ. Chang. 19, 34–44.
Xiong, W., Holman, I., Lin, E.D., Conway, D., Jiang, J.H., Xu, Y.L., Li, Y., 2010. Climate change, water availability and future cereal production in China. Agric. Ecosyst. Environ. 135, 58–69.
Xu, C.H., Xu, Y., 2012. The projection of temperature and precipitation over China under RCP scenarios using a CMIP5 multi-model ensemble. Atmos. Ocean. Sci. Lett. 5, 527–533.
Yao, L., Zheng, H.B., Liu, J.X., He, H., Huang, H., 2014. Current situation and prospect of rice water-saving irrigation technology in China. Chin. J. Ecol. 33, 1381–1387.
Yin, Y.Y., Tang, Q.H., Liu, X.C., Zhang, X.J., 2017. Water scarcity under various socio-economic pathways and its potential effects on food production in the Yellow River basin. Hydrol. Earth Syst. Sci. 21, 791–804.
Zhang, Y., Sun, J.Q., 2012. Model projections of precipitation minus evaporation in China. Acta Meteorol. Sin. 26, 376–388.
Zhang, Q., Sun, P., Singh, V.P., Chen, X.H., 2012. Spatial-temporal precipitation changes (1956–2000) and their implications for agriculture in China. Glob. Planet. Chang. 82–83, 86–95.
Zhang, Y.J., Wang, Y.F., Niu, H.S., 2017. Spatio-temporal variations in the areas suitable for the cultivation of rice and maize in China under future climate scenarios. Sci. Total Environ. 601–602, 518–531.
Zhang, Y.J., Li, Y., Ge, J., Li, G.P., Yu, Z.S., Niu, H.S., 2018a. Correlation analysis between drought indices and terrestrial water storage from 2002 to 2015 in China. Environ. Earth Sci. 77, 462. https://doi.org/10.1007/s12665-018-7651-8.
Zhang, Y.J., Yu, Z.S., Niu, H.S., 2018b. Standardized Precipitation Evapotranspiration Index is highly correlated with total water storage over China under future climate scenarios. Atmos. Environ. 194, 123–133.
Zhao, T.B., Chen, L., Ma, Z.G., 2014. Simulation of historical and projected climate change in arid and semiarid areas by CMIP5 models. Chin. Sci. Bull. 59, 412–429.
Zhu, X.F., Zhao, A.Z., Li, Y.Z., Liu, X.F., 2015. Agricultural irrigation requirements under future climate scenarios in China. J. Arid Land 7, 224–237.